
Long-Tailed Distribution-Aware Router For Mixture-of-Experts in Large Vision-Language Model

Chaoxiang Cai
Zhejiang University
cxc@zju.edu.cn

Longrong Yang
Zhejiang University
longrongyang@zju.edu.cn

Kaibing Chen
Kuaishou Technology
chenkaibing@kuaishou.com

Fan Yang
Kuaishou Technology
yangfan@kuaishou.com

Xi Li*
Zhejiang University
xilizju@zju.edu.cn

Abstract

The mixture-of-experts (MoE), which replaces dense models with sparse architectures, has gained attention in large vision-language models (LVLMs) for achieving comparable performance with fewer activated parameters. Existing MoE frameworks for LVLMs focus on token-to-expert routing (TER), encouraging different experts to specialize in processing distinct tokens. However, these frameworks often rely on the load balancing mechanism, overlooking the inherent distributional differences between vision and language. To this end, we propose a **Long-Tailed Distribution-aware Router** (LTDR) for vision-language TER, tackling two challenges: (1) Distribution-aware router for modality-specific routing. We observe that language TER follows a uniform distribution, whereas vision TER exhibits a long-tailed distribution. This discrepancy necessitates distinct routing strategies tailored to each modality. (2) Enhancing expert activation for vision tail tokens. Recognizing the importance of vision tail tokens, we introduce an oversampling-like strategy by increasing the number of activated experts for these tokens. Experiments on extensive benchmarks validate the effectiveness of our approach.

1 Introduction

Recent advances in large vision-language models (LVLMs) Achiam et al. [2023], MetaAI [2024], which bridge the vision-language gap, have demonstrated strong instruction-following and generalization capabilities. However, real-world deployment requires models to handle diverse tasks simultaneously. Traditional methods that train separate models for per task incur significant redundancy and resource consumption. While Liu et al. [2023a], Chen et al. [2023b], Lu et al. [2024], Bai et al. [2023c] explore the scaling of dataset or model, which still demand substantial resources.

The mixture-of-experts (MoE) Jacobs et al. [1991] is well-suited as it scales trainable parameters to handle diverse tasks while maintaining low inference costs. Dou et al. [2023], Lin et al. [2024a], Dai et al. [2024], Gou et al. [2023] have demonstrated the effectiveness of MoE in model scaling and performance enhancement. For instance, MoE-LLaVA Lin et al. [2024a] achieves comparable performance to LLaVA-7B and LLaVA-13B while activating 3B parameters. The key of MoE is token-to-expert routing (TER). Most implementations Shazeer et al. [2017], Lepikhin et al. [2020] employ trainable routers to predict routing probabilities. To avoid expert overload or underload, existing methods enforce load balancing constraints on TER to make the probability of tokens being allocated to different experts uniform. However, in multi-modal tasks, vision tokens exhibit a

*Corresponding author

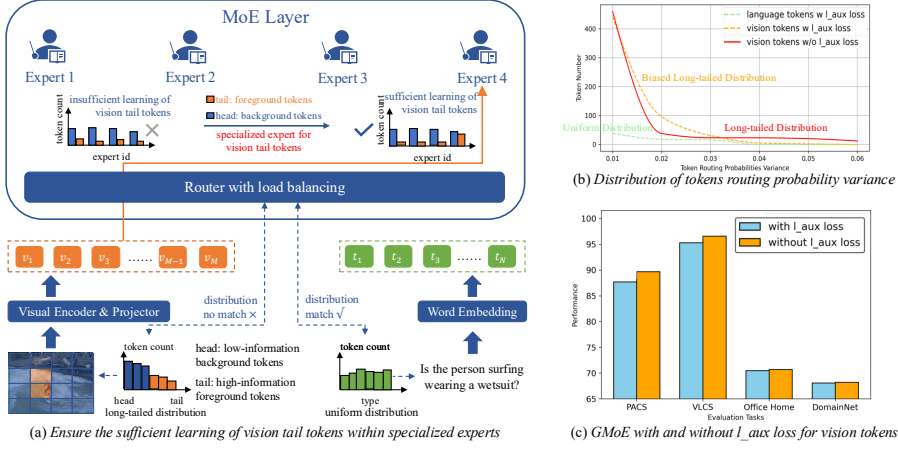


Figure 1: (a) Our goal is to ensure the sufficient learning of vision tail tokens within specialized experts, as head tokens are dense but low-information, while tail tokens are sparse yet high-information. (b) Distribution of TER probability variance. **Language TER with load balancing** shows a uniform distribution, **vision TER without load balancing** exhibits a long-tailed distribution and **vision TER with load balancing** shows a biased long-tailed distribution. (c) GMoE with and without load balancing. Removing load balancing from vision tokens improves performance.

long-tailed distribution Krizhevsky et al. [2017], He et al. [2016] while language tokens exhibit a uniform distribution Vaswani et al. [2017], Devlin et al. [2019]. Indiscriminately using load balancing leads to sub-optimal learning of vision tokens. Specifically, as shown in Fig. 1 (a), vision tokens consist of a large number of low-information background tokens (*i.e.*, the head) and a small number of high-information foreground tokens (*i.e.*, the tail). Load balancing scatters a small number of foreground tokens across different experts, which is detrimental to the correct selection of specialized experts for these tokens that contain important foreground information.

We conduct an in-depth study of this phenomenon. Fig. 1 (b) shows routing probability variance (x-axis) against token count (y-axis), where routing probability variance is defined as the variance of the TER probability distribution. We find that the vision token count exhibits a long-tailed distribution across different probability variances, *i.e.*, most tokens have low probability variances. These tokens are usually background as the router is hard to give confident scores for these low-information background tokens to route to specific experts. In contrast, high-information foreground tokens typically have high variance. As shown in Fig. 1 (b), with load balance, the count of tokens with high variance decreases, indicating that it becomes hard to select specialized experts for foreground tokens. Thus, load balancing impedes the specialized expert selection of these tokens. On the other side, the language token count is uniformly distributed across different probability variances. Thus, language tokens are compatible with load balancing. Fig. 1 (c) shows that removing load balancing from vision tokens enhances vision performance. Based on the above observations, our goal is to ensure the sufficient learning of vision tail tokens within the specialized expert as shown in Fig. 1 (a).

To ensure the sufficient learning of vision tail tokens, we propose the **Long-Tailed Distribution-aware Router** (LTDR) to address two challenges: (1) *Distribution-aware Router for Modality-Specific Routing*. Increasing the variance of routing probabilities allows vision tokens, especially vision tail tokens, to focus on specialized experts. To this end, we retain load balancing for language TER, as it aligns well with the uniform language token distribution. Instead, for vision TER, we abandon load balancing to adaptively align with the long-tailed vision token distribution. (2) *Enhancing Expert Activation for Vision Tail Tokens*. We increase the number of activated experts for vision tail tokens, using an oversample-like strategy to enhance fault tolerance in expert selection. Experiments on vision-language and vision-only benchmarks demonstrate that LTDR enhances visual understanding.

Our contribution can be summarized as follows:

- Given the different distributions of vision and language tokens, we reveal the negative impact of load balancing on vision tokens, *i.e.*, insufficient learning of important vision tail tokens.

To adapt to the long-tailed vision token distribution, we propose to adjust the conventional load balancing mechanism for different modality.

- We propose a long-tailed distribution-aware router (LTDR) for modality-specific routing, and enhance expert activation for vision tail tokens.
- Extensive experimental results on both vision-language and vision-only benchmarks fully demonstrate the effectiveness of our proposed method.

2 Related Work

2.1 Large Vision-Language Models

The remarkable success of large language models (LLMs) has significantly accelerated progress in vision-language research Lin et al. [2024a]. LVLMs like GPT-4 Achiam et al. [2023] and LLaVA Liu et al. [2023a] have become a prominent research focus, employing frozen visual encoders and trainable visual projectors to bridge the modality gap between vision and language. These models encode visual inputs into LLMs-compatible representations, enabling seamless multi-modal integration. Current research primarily explores dataset scaling Zhang et al. [2023] and parameter-efficient adaptation methods Houldsby et al. [2019], Lester et al. [2021], Hu et al. [2021], Ye et al. [2023] to enhance efficiency and scalability. However, LVLMs still face critical challenges, including limited task generalization and rapidly escalating inference costs with parameter growth. MoE paradigm has emerged as a promising solution, offering efficient parameter scaling while maintaining computational tractability.

2.2 Long-Tailed Distribution

Real-world data naturally exhibits a long-tailed distribution, where a few dominant classes contain abundant samples while most classes suffer from severe data scarcity Kang et al. [2020], Menon et al. [2020], Liu et al. [2019], Cui et al. [2019]. This inherent class imbalance significantly impairs deep learning model training. Current mitigation approaches typically fall into resampling Buda et al. [2018], Han et al. [2005], reweighting Lin et al. [2017], Wang et al. [2017], and logits adjustment Ren et al. [2020], Hong et al. [2021]. In vision-language tasks, the challenge intensifies as the long-tailed distribution manifests at both samples and tokens, creating compounded difficulties for effective model training and optimal performance.

2.3 Mixture-of-Experts

MoE Jacobs et al. [1991], Shazeer et al. [2017], Lepikhin et al. [2020] composed of an expert group has shown the potential in scaling up models. Fine-grained MoE frameworks Dai et al. [2024], Bai et al. [2023a] expand experts by splitting the FFN intermediate hidden dimension. MoE based LVLMs Lin et al. [2024a], Chen et al. [2024b] have achieved notable progress on vision-language tasks.

Traditional MoE Shazeer et al. [2017], Lepikhin et al. [2020] employs trainable linear layers for routing probability prediction. Task routing Jain et al. [2024], Gururangan et al. [2021], Zhou et al. [2024] assign task-specific tokens to predetermined experts, while cluster routing Dou et al. [2023], Gou et al. [2023] groups feature-similar tokens to fixed experts. Dynamic routing Huang et al. [2024], Guo et al. [2024] adaptively adjusts expert numbers to reduce hyper-parameter constraints. Recent advances have introduced more sophisticated techniques, including multi-gate for task relationship modeling Ma et al. [2018], STGC for gradient conflicts mitigating Yang et al. [2024], and Lory for sequential routing Zhong et al. [2024]. Nevertheless, existing methods neglect the issue of routing under long-tailed distribution, which are normal in practical applications.

To our best knowledge, SHIKE Jin et al. [2023] and RIDE Wang et al. [2020] focus on sample-level long-tailed distribution. However, they only use traditional routing strategies to mitigate model bias, without introducing innovations in routing mechanisms. Our LTDR tackles the scenario of token-level long-tailed distributions in multi-modal. Besides, LTDR can process data from diverse modalities through distinct routing mechanisms, thereby offering a more comprehensive solution to this complex problem.

3 Methodology

3.1 Preliminaries

Large Vision-Language Models. LVLMs integrate the capabilities of LLMs with advanced vision processing technologies, enabling vision-language understanding and generation. As shown in Fig. 1 (a), the text input is first transformed through a word embedding, which projects the text \mathbf{t} into a continuous vector space, resulting in the language token sequence $\mathcal{T} = [t_1, t_2, \dots, t_N] \in \mathbb{R}^{N \times D}$. N means the sequence length of language tokens, and D denotes the hidden layer size of the LLM.

Similarly, the RGB image input $\mathbf{v} \in \mathbb{R}^{H \times W \times 3}$, where H , W , and 3 denote the height, width, and channels of the image at its original resolution, the visual encoder processes the image to extract a sequence of vision tokens $\mathcal{Z} = [z_1, z_2, \dots, z_M] \in \mathbb{R}^{M \times C}$. M is the sequence length of vision tokens, and C is the hidden size of the visual encoder. To align vision tokens with language tokens in the same vector space, a visual projection layer is employed to map $\mathcal{Z} \in \mathbb{R}^{M \times C}$ to $\mathcal{V} = [v_1, v_2, \dots, v_M] \in \mathbb{R}^{M \times D}$, where D matches the hidden layer size of the LLM. This alignment ensures that both vision and language can be processed jointly by the subsequent layers of the model.

Subsequently, vision and language tokens are concatenated and fed into the LLM. The LLM consists of layers of multi-head self-attention (MSA) and feed-forward network (FFN), with layer normalization (LN) and residual connection applied to stabilize training and enhance performance. As shown in Eq. 1 ~ Eq. 4, where L is the layer number of LLM, the LVLM achieve a deep understanding of the relationships between vision and language, enabling effective performance on vision-language tasks.

$$\mathbf{x}_0 = [v_1, v_2, \dots, v_M, \dots, t_1, t_2, \dots, t_N], \quad (1)$$

$$\mathbf{x}'_\ell = \text{MSA}(\text{LN}(\mathbf{x}_{\ell-1})) + \mathbf{x}_{\ell-1}, \ell \in \{1, \dots, L\}, \quad (2)$$

$$\mathbf{x}_\ell = \text{FFN}(\text{LN}(\mathbf{x}'_\ell)) + \mathbf{x}'_\ell, \ell \in \{1, \dots, L\}, \quad (3)$$

$$\mathcal{Y} = \text{LN}(\mathbf{x}_L), \quad (4)$$

The output of the LVLM is optimized through a generative loss in an auto-regressive manner. Given an image and its corresponding instruction text, the LVLM aims to generate the output text sequence $\mathcal{Y} = [y_1, y_2, \dots, y_O] \in \mathbb{R}^{O \times D}$ by progressively prediction, where O is the sequence length of the text output. The loss function is defined in Eq. 5, $\mathcal{Y}_{<i}$ indicates the output sequence before token y_i , θ denotes the trainable parameters of the model. We only calculate the loss for the generated text.

$$\mathcal{L}_{\text{regressive}} = - \sum_{i=1}^O \log p(y_i \mid \mathcal{V}, \mathcal{T}, \mathcal{Y}_{<i}, \theta), \quad (5)$$

Mixture-of-Experts. We replace the FFN as MoE, following MoE-LLaVA Lin et al. [2024a]. A MoE layer contains multiple FFNs, denoted as an experts ensemble $\mathcal{E} = [e_1, e_2, \dots, e_K]$, K is the number of experts. The router implements a linear layer to predict the routing probability of assigning tokens to experts. As shown in Eq. 6, the router produces weight logits $f(\mathbf{x}) = \mathbf{W} \cdot \mathbf{x}$, which are normalized by the softmax function. The matrix $\mathbf{W} \in \mathbb{R}^{D \times K}$ denotes the lightweight trainable parameters for routing, $\mathcal{P}(\mathbf{x})_i$ is the routing score of the input \mathbf{x} for the i -th expert. The final output in Eq. 7 is computed as a weighted sum of the outputs from the Top- k experts with the highest softmax probabilities. $\mathcal{E}(\mathbf{x})_i$ is the output of the i -th expert, and the weight for each expert is determined by its routing score.

$$\mathcal{P}(\mathbf{x})_i = \frac{e^{f(\mathbf{x})_i}}{\sum_{j=1}^K e^{f(\mathbf{x})_j}}, \quad (6)$$

$$\text{MoE}(\mathbf{x}) = \sum_{i=1}^k \mathcal{P}(\mathbf{x})_i \cdot \mathcal{E}(\mathbf{x})_i, \quad (7)$$

Due to the presence of multiple experts, it is necessary to impose expert load balancing constraints on the MoE layer. Traditional methods Lin et al. [2024a], Yang et al. [2024] incorporate differentiable load balancing loss Fedus et al. [2022] into each MoE layer to encourage experts to handle tokens in

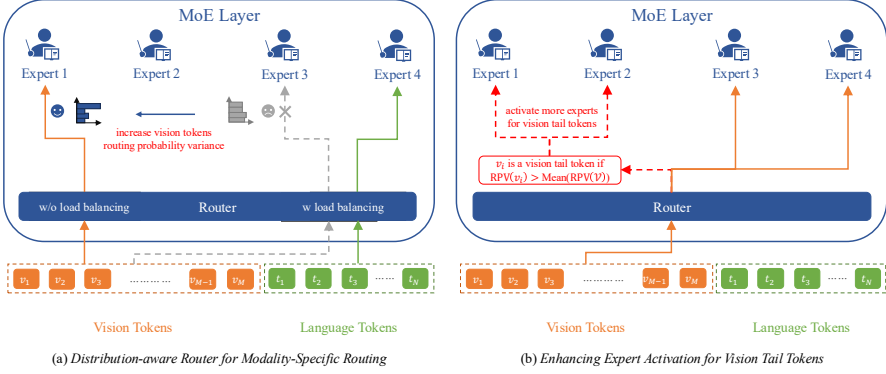


Figure 2: (a) We use a distribution-aware router for modality-specific routing, allowing vision and language to be routed with different expert loads to adapt to their respective modality distributions. (b) We define the head and tail tokens of vision, and enhance expert activation for vision tail tokens, enabling an oversample-like method to make experts process important vision tail tokens sufficiently.

a balanced manner. As shown in Eq. 8, \mathcal{F}_i is the fraction of tokens processed by expert \mathcal{E}_i , and \mathcal{G}_i is the average routing probability of expert \mathcal{E}_i .

$$\mathcal{L}_{\text{balancing}} = K \cdot \sum_{i=1}^K \mathcal{F}_i \cdot \mathcal{G}_i, \quad (8)$$

Our Method LTDR. Since language tokens follow a uniform distribution, while vision tokens exhibit a long-tailed distribution, we focus on optimizing vision-language TER to make experts handle different distributional modality tokens effectively. We find that the load balancing mechanism leads to the scattered vision tail tokens in experts, impeding the learning of specialized experts. Therefore, as illustrated in Fig. 2, our method consists of two sub-modules: (1) Distribution-aware router for modality-specific routing. We retain load balancing for language TER as it aligns with the uniform distribution of language tokens, while discard load balancing for vision TER to adaptively align with the long-tailed distribution of visual tokens. Without load balancing, vision tokens, especially vision tail tokens, exhibit higher routing probability variance, enabling specialized expert selection. (2) Enhancing expert activation for vision tail tokens. Given the high importance of vision tail tokens, we define the head and tail tokens of vision, and increase the number of activated experts for vision tail tokens, achieving an oversample-like strategy to improve fault tolerance and learning effectiveness.

3.2 Distribution-aware Router for Modality-Specific Routing

Existing MoE frameworks on modality differences fall into modality-aware Nguyen et al. [2024], Chen et al. [2024a], Lin et al. [2024b] and distribution-aware Jin et al. [2023], Wang et al. [2020]. HMoE Nguyen et al. [2024] and MoMa Lin et al. [2024b] center on modalities by using a hierarchical MoE and modality-specific expert groups, while SHIKE Jin et al. [2023] and RIDE Wang et al. [2020] focus on long-tailed distribution by enhancing expert diversity and reducing dynamic routing. These methods are constrained by load balancing (Eq. 8), without considering modality token distribution differences.

Vaswani et al. [2017], Devlin et al. [2019], Krizhevsky et al. [2017], He et al. [2016] has shown that language follows a uniform distribution, whereas vision exhibits a long-tailed distribution. This divergence stems from the characteristics of vision, which contains a few foreground patches and a large number of background patches. Radford et al. [2021], Kim et al. [2021] also emphasize that the structural and semantic differences between vision and language necessitate tailored processing. To this end, we optimize the vision-language TER distribution (Eq. 6) for vision and language.

Load balancing conflicts with the long-tailed vision distribution, an intuitive way is to release vision tokens from load balancing to increase their routing probability variance (RPV). As shown in Eq. 9, for a vision token $v_i \in \mathcal{V}$, its routing probabilities $\mathcal{P}(v_i) \in \mathbb{R}^K$, and $\text{RPV}(v_i)$ is its variance of $\mathcal{P}(v_i)$. The number of vision head tokens is sufficient to generalize across various experts, resulting

in averaged routing probability (low RPV). While the limited number of vision tail tokens, if forced to distributed evenly across experts, would lead to poor generalization. Therefore, a distribution-aware router is essential to enable modality-specific routing to benefit the learning of experts for vision tokens. We modify the traditional $\mathcal{L}_{\text{balancing}}$ in Eq. 10, where \mathcal{T} means the language token sequence.

$$\text{RPV}(v_i) = \text{Variance}(\mathcal{P}(v_i)), \quad (9)$$

$$\mathcal{L}_{\text{balancing}} = \sum_{i=1}^K \mathcal{F}_i(\mathcal{T}) \cdot \mathcal{G}_i(\mathcal{T}) \quad (10)$$

In this framework, language tokens maintain their original routing, while vision tokens are released from the constraint of load balancing. This enables vision tokens, especially vision tail tokens, which represent information-rich content, to undergo specialized expert processing. As shown in Fig. 2 (a), by enhancing the RPV of vision tokens, these tokens can be allocated to specialized experts instead of being uniformly distributed, facilitating more precise and efficient learning.

3.3 Enhancing Expert Activation for Vision Tail Tokens

Given the high importance of vision tail tokens, we seek to enhance their processing for sufficient expert learning. However, the complexity and training instability introduced by long-tailed tokens necessitate a simple yet effective solution. Since the input and output token sequence lengths fix before and after each FFN layer, traditional undersampling or oversampling methods are impractical for adjusting head or tail token quantities. To address this, we employ an oversample-like strategy to enhance the expert learning and processing for vision tail tokens without introducing new tokens.

As illustrated in Fig. 2 (b), our innovation lies in defining and identifying vision tail tokens and activating more experts to learn and process vision tail tokens. First of all, we define whether a vision token $v_i \in \mathcal{V}$ is a vision head token or vision tail token by the following Eq. 11.

$$\text{Type}(v_i) = \text{tail, if } \text{RPV}(v_i) > \text{Mean}(\text{RPV}(\mathcal{V})) \quad (11)$$

Where $\text{Mean}(\text{RPV}(\mathcal{V}))$ represents the mean value of $\text{RPV}(\mathcal{V}) \in \mathbb{R}^M$. We serve vision tokens with larger RPV than the $\text{Mean}(\text{RPV}(\mathcal{V}))$ of total vision token sequence as vision tail tokens, and others are considered as heads. RPV reflects TER distribution. Vision tail tokens exhibit higher RPV than head tokens, as they are processed by specialized experts. We use mean RPV as the threshold for vision tail token recognition, as it can already filter out most of vision head tokens. Subsequently, we route identified vision tail tokens to more experts than originally allocated, resulting in a modified version of Eq. 7 tailored for vision tail tokens in Eq. 12:

$$\text{MoE}(x) = \begin{cases} \sum_{j=1}^a \mathcal{P}(x)_j \cdot \mathcal{E}(x)_j, & \text{vision tail token} \\ \sum_{j=1}^k \mathcal{P}(x)_j \cdot \mathcal{E}(x)_j, & \text{vision head \& language token} \end{cases} \quad (12)$$

Where vision tail tokens are processed by all more experts ($k < a \leq K$), $a = K$ in this work. In this way, vision tail tokens can be further learned and processed by more experts to mitigate the problems caused by expert incorrect routing and enhance the fault tolerance caused by expert selection errors.

4 Experiments

4.1 Experimental Setup

Benchmarks. Our goal is to study the vision TER within the MoE. To ensure a robust evaluation of our approach, we perform extensive experiments encompassing both vision-language and vision-only tasks. Please see Appendix A.1 for detailed benchmarks. These benchmarks provide a comprehensive evaluation framework, ensuring our approach is rigorously tested across diverse capabilities.

Baselines. We employ MoE-LLaVA Lin et al. [2024a] for vision-language tasks and GMoE Li et al. [2022] for vision-only tasks. MoE-LLaVA enhances LVLMs by MoE and introduce a three-stage

training strategy. In the instruction tuning phase, the training is exclusively focused on the MoE component. The model adopts a 4Top2 selection mechanism, that is, among the four experts in total, only the two most relevant experts are activated to process each token. GMoE is designed for vision domain generalization. It enhances the pre-trained ViT-S/16 model Dosovitskiy et al. [2020] through a sparse MoE architecture, aiming to strengthen the model’s ability to generalize effectively across data from diverse domains.

Configurations. Building on the above benchmarks and baselines, we introduce a long-tailed distribution-aware router to enhance vision TER. For the language model backbone in vision-language tasks, we use StableLM-1.6B, Qwen-1.8B, and Phi2-2.7B, following MoE-LLaVA. The visual encoder is CLIP, with the hyper-parameters of $\mathcal{L}_{\text{balancing}}$, $\alpha = 0.01$. For the vision model backbone in vision-only tasks, we adhere to GMoE by using the pre-trained ViT-S/16 model as the backbone. Our routing strategy is implemented at each **batch**. Please see Appendix A.2 for detailed configurations.

4.2 Comprehensive Evaluation

Vision-Language Main Evaluation. As shown in Tab. 1, we evaluate the performance of our method on three image question-answering benchmarks and four benchmark toolkits, reporting both accuracy and the parameter of LLMs. Our method demonstrates robust image understanding capabilities, showing superior performance compared to MoE-LLaVA. Specifically, we achieve average improvements of 1.2%, 0.4%, and 0.5% over StableLM-1.6B, Qwen-1.8B, and Phi2-2.7B models, respectively. These results highlight the effectiveness of our approach. Additionally, the consistent gains across different model sizes underscore the scalability and adaptability of our method.

Table 1: **Comparison between different LVLMs on vision-language benchmarks.** “L”, “V”, “S”, “Q”, “P”, “M” and “I” respectively represent LLaMA Touvron et al. [2023], Vicuna Chiang et al. [2023], StableLM Bellagente et al. [2024], Qwen Bai et al. [2023b], Phi-2 Javaheripi et al. [2023], MobileLLaMA Chu et al. [2023] and IDEFICS Laurençon et al. [2023]. Evaluation benchmarks include GQA Hudson and Manning [2019]; SQA^T: ScienceQA-IMG Lu et al. [2022]; VQA^T: TextVQA Singh et al. [2019]; POPE Li et al. [2023]; MME Fu et al. [2023]; MMB: MMBench Liu et al. [2023b] and MM-Vet Yu et al. [2023]. * indicates that there is some overlap in the training data. Sparse models use the configure 4Top2. We calculate the average performance “Avg” across all datasets except for MME.

Method	LLM	GQA	SQA ^T	VQA ^T	POPE	MME	MMB	MM-Vet	Avg
<i>Dense Model</i>									
I-80B Laurençon et al. [2023]	65B	45.2	-	30.9	-	-	54.5	-	-
LLaVA-1.5 Liu et al. [2023a]	L-13B	63.3*	71.6	61.3	85.9	1531.3	67.7	35.4	64.2
LLaVA-1.5 Liu et al. [2023a]	V-7B	62.0*	66.8	58.2	85.9	1510.7	64.3	30.5	61.3
Qwen-VL Bai et al. [2023c]	Q-7B	59.3*	67.1	63.8	-	-	38.2	-	-
TinyGPT-V Yuan et al. [2023]	P-2.7B	33.6*	-	-	-	-	-	-	-
MobileVLM Chu et al. [2023]	M-2.7B	59.0*	61.0	47.5	84.9	1288.9	59.6	-	-
LLaVA-Phi Zhu et al. [2024]	P-2.7B	-	68.4	48.6	85.0	1335.1	59.8	28.9	-
<i>Sparse Model</i>									
MoE-LLaVA-4Top2	S-1.6B	60.3*	62.6	50.1	85.7	1318.2	60.2	26.9	57.6
Our Method	S-1.6B	61.1*	63.4	51.1	86.6	1363.5	60.6	29.9	58.8
MoE-LLaVA-4Top2	Q-1.8B	61.5*	63.1	48.0	87.0	1291.6	59.7	25.3	57.4
Our Method	Q-1.8B	61.6*	62.8	48.9	87.2	1334.2	60.5	25.5	57.8
MoE-LLaVA-4Top2	P-2.7B	61.4*	68.5	51.4	86.3	1423.0	65.2	34.3	61.2
Our Method	P-2.7B	62.2*	68.5	52.0	86.7	1440.8	66.7	34.0	61.7

Table 2: **Comparison between different large vision models (LVMs) on vision-only benchmarks.** Evaluation benchmarks include PACS Li et al. [2017], VLCS Albuquerque et al. [2019], Office-Home Venkateswara et al. [2017] and DomainNet Peng et al. [2019]. KTopk means k experts out of K experts are activated. We calculate the average performance “Avg”.

Method	PACS			VLCS			Office-Home			DomainNet			Avg
	4Top1	4Top2	6Top2	4Top1	4Top2	6Top2	4Top1	4Top2	6Top2	4Top1	4Top2	6Top2	
GMoE	86.7	88.9	87.6	96.8	92.5	96.5	70.1	70.5	71.0	67.6	68.5	68.2	80.4
DYNAMIC	-	-	87.6	-	79.4	-	-	-	73.6	-	48.2	-	-
Our Method	86.8	90.1	92.1	97.1	95.7	96.9	70.2	70.6	71.4	67.8	68.5	68.3	81.3

Vision-Only Main Evaluation. As shown in Tab. 2, we also evaluate the performance of our method on four vision-only benchmarks, which are specifically designed to assess domain generalization and adaptation capabilities across diverse visual domains. To thoroughly analyze the generalization ability of our method, we report results under different settings, including 4Top1, 4Top2, and 6Top2 configurations. With the integration of our proposed LTDR, GMoE demonstrates consistent improvements across all benchmarks and settings, achieving an average performance gain of 0.9% compared to previous results. This improvement underscores the effectiveness of LTDR in enhancing the vision model’s capability to generalize to unseen domains and adapt to varying data distributions. Besides, in vision-only tasks, our approach outperforms the recent MoE framework DYNAMIC Guo et al. [2024].

4.3 Ablation Study

We conduct ablations on MoE-LLaVA-4Top2 with StableLM-1.6B model on vision-language benchmarks in Tab. 3. First, a distribution-aware router (DAR) for modality-specific routing improves performance. Second, enhancing expert activation (EEA) for vision tail tokens boosts model accuracy. The results of removing language load balancing (LLB) and all load balancing (ALB) indicate that removing LLB is negligible. These findings collectively highlight the critical roles of DAR and EEA.

Additionally, we count the running time on MoE-LLaVA-4Top2 with StableLM-1.6B model in Tab. 4. Surprisingly, although our method introduces more experts for vision tail tokens, its training time does not increase significantly compared to the baseline. The inference time is lower than the baseline while the performance is better. We guess this is due to DeepSpeed MoE’s parallel computing ².

We also analyze the proportion of vision tail tokens and find that only about 13% vision tokens (each image yields 576 tokens) are defined as vision tail tokens. Therefore, EEA is effective not because more experts are introduced, but because the visual tail tokens are better learned and processed.

Table 3: **Ablations on MoE-LLaVA with S-1.6B model on vision-language benchmarks.**

Method	GQA	SQA ¹	VQA ^T	POPE	MME	MMB	MM-Vet	Avg
MoE-LLaVA-4Top2	60.3*	62.6	50.1	85.7	1318.2	60.2	26.9	57.6
+ DAR	61.1*	62.3	51.2	86.6	1324.3	59.9	27.9	58.2
+ EEA	61.1*	61.3	51.1	86.6	1324.5	61.1	28.5	58.3
+ DAR&EEA (LTDR)	61.1*	63.4	51.1	86.6	1363.5	60.6	29.9	58.8
- LLB	60.9*	62.0	50.3	85.8	1254.1	60.1	27.9	57.8
- ALB	61.1*	61.9	51.3	86.2	1324.2	60.4	28.5	58.2

Table 4: **Running time on MoE-LLaVA with S-1.6B model on vision-language benchmarks.**

Method	Training Time (s)	Inference Time (s)							Avg
		GQA	SQA ¹	VQA ^T	POPE	MME	MMB	MM-Vet	
MoE-LLaVA-4Top2	24056	1771	285	1265	1269	363	603	310	838
Our method	24227	1698	301	1057	1116	317	595	310	770

4.4 Comparison Study

Different Routing Strategies. We compare our routing strategy with popular strategies in Tab. 5. Task routing Gururangan et al. [2021], Jain et al. [2024], Zhou et al. [2024] routes by task type. Cluster routing Dou et al. [2023], Gou et al. [2023] groups instruction embeddings via K-means for routing. Instruct routing Chen et al. [2023a] predicts routing scores via instance-level instruction token representations. Dynamic routing Huang et al. [2024], Guo et al. [2024] adaptively adjusts expert numbers, while STGC Yang et al. [2024] routes tokens without conflicts. Please see Appendix A.3 for detailed routing strategy implements. Our method consistently outperforms others: It slightly surpasses DYNAMIC and STGC on GQA. On SQA¹, TASK and CLUSTER excel, with our method close behind. It achieves top performance on VQA^T, outperforms STGC and CLUSTER on POPE, and surpasses STGC and DYNAMIC on MME. On MM-Vet, our method also leads. Overall, our

²<https://github.com/deepspeedai/DeepSpeed>.

Table 5: **Comparison between different routing strategies on vision-language benchmarks.** TASK, CLUSTER, INSTRUCT, DYNAMIC, and STGC denote task routing Gururangan et al. [2021], Jain et al. [2024], Zhou et al. [2024], cluster routing Dou et al. [2023], Gou et al. [2023], instruction routing Chen et al. [2023a], dynamic routing Huang et al. [2024], Guo et al. [2024], and conflicts mitigation routing Yang et al. [2024], respectively. All experiments are conducted on the MoE-LLaVA-4Top2 with StableLM-1.6B model. The best and second-best results are marked with **boldface** and underline.

Method	GQA	SQA ^I	VQA ^T	POPE	MME	MMB	MM-Vet	Avg
MoE-LLaVA-4Top2	60.3*	62.6	50.1	85.7	1318.2	60.2	26.9	57.6
+ TASK	58.2*	63.7	49.2	81.5	1306.3	59.5	25.2	56.2
+ CLUSTER	57.0*	63.7	50.3	<u>86.1</u>	1312.8	<u>62.3</u>	27.3	57.8
+ INSTRUCT	58.1*	63.2	50.0	85.9	1338.8	61.5	26.6	57.5
+ DYNAMIC	<u>61.0</u> *	62.1	49.2	85.7	1320.4	62.4	<u>28.2</u>	<u>58.1</u>
+ STGC	60.9*	62.6	<u>50.7</u>	85.9	<u>1355.1</u>	60.7	<u>28.2</u>	<u>58.1</u>
+ LTDR (Ours)	61.1 *	<u>63.4</u>	51.1	86.6	1363.5	60.6	29.9	58.8

Table 6: **Comparison with the “Shared Experts + Routed Experts” strategy of DeepSeekMoE** Dai et al. [2024] **on vision-language benchmarks.** $S_s + R_r$ denotes S shared expert(s) of size s combined with R routing experts of size r. All experiments are conducted on the MoE-LLaVA-4Top2 with StableLM-1.6B model. The best and second-best results are marked with **boldface** and underline.

Method	GQA	SQA ^I	VQA ^T	POPE	MME	MMB	MM-Vet	Avg
MoE-LLaVA-4Top2 (4 _{1.0})	60.3*	62.5	50.1	85.7	1318.2	60.2	26.9	57.6
+ 1 _{1.0} + 3 _{1.0}	61.1 *	62.5	50.4	86.2	<u>1330.1</u>	<u>57.6</u>	27.9	57.6
+ 1 _{1.0} + 12 _{0.25}	60.4*	62.7	<u>50.4</u>	<u>86.2</u>	1327.1	<u>57.6</u>	27.9	57.5
+ 1 _{1.0} + 16 _{0.25}	60.9*	<u>62.8</u>	49.9	<u>86.2</u>	1318.5	58.7	<u>28.1</u>	57.7
+ LTDR (4 _{1.0})	61.1 *	63.4	51.1	86.6	1363.5	60.6	29.9	58.8

proposed LTDR achieves the highest average score, demonstrating superior performance across vision-language tasks.

Comparison with DeepSeekMoE. We also compare with DeepSeekMoE Dai et al. [2024] in Tab. 6, which divides K original experts into mK finer experts and activates mk finer experts. For activated mk finer experts, they are further divided as k_s shared experts to make shared learning and k_r routing experts to achieve specialized learning. The evaluation under three settings (1_{1.0} + 3_{1.0}, 1_{1.0} + 12_{0.25}, 1_{1.0} + 16_{0.25}) illustrates that DeepSeekMoE underperforms on vision-language benchmarks despite increased specialization, even regressing in some cases. This supports our hypothesis that vision and language TER differ, highlighting the need for tailored vision-language routing strategies.

Different Vision Token Selection Strategies in Enhancing Expert Activation. For the stage of EAA in LTDR, we choose vision tail tokens (VTT) whose RPV exceeds the mean RPV of all vision tokens. We compare ours with other two strategies in Tab. 7: Vision head tokens (VHT), the inverse of our VTT, whose RPV is below the mean RPV of all vision tokens. As a result, VHT selects a larger proportion of tokens (87%) for EEA compared to VTT. Instruction-aware Tokens (IAT). We utilize the attention scores between the instruction and vision tokens to identify the top 15% of vision tokens for EEA. Ensuring that the selected tokens are most relevant to the given instructions.

As shown in Tab.7, enhancing expert activations for vision head tokens can also improve LVLMs’ ability to learn visual information, although its benefits are not as significant as those of VTT. Additionally, selecting too many tokens will increase its time cost of training. The influence of IAT is minimal. We guess that the instruction-aware method is influenced by noise from both visual and textual information, which may prevent it from reliably identifying important visual tokens.

More comparison studies. For more comprehensive comparison studies that are not be included, we provide detailed analyses in the Appendix. These supplementary investigations include but not limited to: **Comparative Analysis with Modality-aware MoE Frameworks** (Appendix B.1), where we benchmark our approach against modality-aware MoE architectures like MoMa Lin et al. [2024b]. **Quantitative Evaluation of Object Hallucination Effects** (Appendix B.2), systematically assessing generation reliability across different model configurations; **Expert Token Loading Analysis** (Appendix C), revealing the expert token loading under our method. This extended content provides critical supporting evidence for our methodological choices and performance claims.

Table 7: **Different Vision Token Selection Strategies in Enhancing Expert Activation.** All experiments are conducted on the MoE-LLaVA-4Top2 with StableLM-1.6B model.

Method	GQA	SQA ^I	VQA ^T	POPE	MME	MMB	MM-Vet	Avg
MoE-LLaVA-4Top2	60.3*	62.6	50.1	85.7	1318.2	60.2	26.9	57.6
VHT	61.0*	62.0	50.3	86.3	1310.9	60.3	27.8	58.0
IAT	60.8*	61.0	50.8	87.0	1307.8	59.7	26.9	57.7
VTT (Ours)	61.1*	63.4	51.1	86.6	1363.5	60.6	29.9	58.8

5 Conclusion and Limitation

We reveal the distinct token-to-expert routing (TER) distributions in vision-language tasks: language TER follows a uniform distribution, while vision TER exhibits a long-tailed distribution. This challenges the conventional load balancing mechanism in MoE: experts should receive an equal number of tokens to avoid a small number of experts gaining a disproportionately large share of preferences by the router. To address this, we propose a **Long-Tailed Distribution-aware Router** (LTDR) for vision-language TER, solving two key issues: (1) Distribution-aware router for modality-specific routing. We retain the load balancing mechanism for language TER but relax it for vision TER, enabling important vision tail tokens to be routed to specialized experts. (2) Enhancing expert activation for vision tail tokens. Recognizing the importance of vision tail tokens, we employ an oversampling-like strategy, which increases the number of activated experts to ensure their thorough processing. To verify the effectiveness of our LTDR, we conduct extensive experiments on both vision-language and vision-only benchmarks. The experimental results validate our approach.

As the vision tail tokens are only identified in one batch of vision tokens in each iteration, it will inevitably misjudge some unimportant vision tokens as vision tail tokens, affecting the model’s reception of key information. Therefore, although it has been demonstrated that the proposed solution can solve the expert specialization problem of vision tail tokens by strengthening vision tail token routing, the solution still has room for improvement because the identification of vision tail tokens is challenging. In the future, it may be an interesting direction to explore whether the vision tail tokens and their optimal experts can be determined from an optimization perspective.

References

Josh Achiam, Steven Adler, Sandhini Agarwal, Lama Ahmad, Ilge Akkaya, Florencia Leoni Aleman, Diogo Almeida, Janko Altenschmidt, Sam Altman, Shyamal Anadkat, et al. Gpt-4 technical report. *arXiv preprint arXiv:2303.08774*, 2023.

Isabela Albuquerque, João Monteiro, Mohammad Darvishi, Tiago H Falk, and Ioannis Mitliagkas. Generalizing to unseen domains via distribution matching. *arXiv preprint arXiv:1911.00804*, 2019.

Jinze Bai, Shuai Bai, Yunfei Chu, Zeyu Cui, Kai Dang, Xiaodong Deng, Yang Fan, Wenbin Ge, Yu Han, Fei Huang, Binyuan Hui, Luo Ji, Mei Li, Junyang Lin, Runji Lin, Dayiheng Liu, Gao Liu, Chengqiang Lu, Keming Lu, Jianxin Ma, Rui Men, Xingzhang Ren, Xuancheng Ren, Chuanqi Tan, Sinan Tan, Jianhong Tu, Peng Wang, Shijie Wang, Wei Wang, Shengguang Wu, Benfeng Xu, Jin Xu, An Yang, Hao Yang, Jian Yang, Shusheng Yang, Yang Yao, Bowen Yu, Hongyi Yuan, Zheng Yuan, Jianwei Zhang, Xingxuan Zhang, Yichang Zhang, Zhenru Zhang, Chang Zhou, Jingren Zhou, Xiaohuan Zhou, and Tianhang Zhu. Qwen technical report. *arXiv preprint arXiv:2309.16609*, 2023a.

Jinze Bai, Shuai Bai, Yunfei Chu, Zeyu Cui, Kai Dang, Xiaodong Deng, Yang Fan, Wenbin Ge, Yu Han, Fei Huang, et al. Qwen technical report. *arXiv preprint arXiv:2309.16609*, 2023b.

Jinze Bai, Shuai Bai, Shusheng Yang, Shijie Wang, Sinan Tan, Peng Wang, Junyang Lin, Chang Zhou, and Jingren Zhou. Qwen-vl: A versatile vision-language model for understanding, localization, text reading, and beyond. *arXiv preprint arXiv:2308.12966*, 2023c.

Marco Bellagente, Jonathan Tow, Dakota Mahan, Duy Phung, Maksym Zhuravinskyi, Reshinth Adithyan, James Baicoianu, Ben Brooks, Nathan Cooper, Ashish Datta, et al. Stable lm 2 1.6 b technical report. *arXiv preprint arXiv:2402.17834*, 2024.

Mateusz Buda, Atsuto Maki, and Maciej A Mazurowski. A systematic study of the class imbalance problem in convolutional neural networks. *Neural networks*, 106:249–259, 2018.

Junyi Chen, Longteng Guo, Jia Sun, Shuai Shao, Zehuan Yuan, Liang Lin, and Dongyu Zhang. Eve: efficient vision-language pre-training with masked prediction and modality-aware moe. In *Proceedings of the AAAI Conference on Artificial Intelligence*, volume 38, pages 1110–1119, 2024a.

Shaoxiang Chen, Zequn Jie, and Lin Ma. Llava-mole: Sparse mixture of lora experts for mitigating data conflicts in instruction finetuning mllms. *arXiv preprint arXiv:2401.16160*, 2024b.

Z Chen, Z Wang, Z Wang, H Liu, Z Yin, S Liu, L Sheng, W Ouyang, Y Qiao, and J Shao. Octavius: mitigating task interference in mllms via moe 2023. *arXiv preprint arXiv:2311.02684*, 2023a.

Zhe Chen, Jiannan Wu, Wenhui Wang, Weijie Su, Guo Chen, Sen Xing, Muyan Zhong, Qinglong Zhang, Xizhou Zhu, Lewei Lu, Bin Li, Ping Luo, Tong Lu, Yu Qiao, and Jifeng Dai. Internvl: Scaling up vision foundation models and aligning for generic visual-linguistic tasks. *arXiv preprint arXiv:2312.14238*, 2023b.

Wei-Lin Chiang, Zhuohan Li, Ziqing Lin, Ying Sheng, Zhanghao Wu, Hao Zhang, Lianmin Zheng, Siyuan Zhuang, Yonghao Zhuang, Joseph E Gonzalez, et al. Vicuna: An open-source chatbot impressing gpt-4 with 90%* chatgpt quality. See <https://vicuna.lmsys.org> (accessed 14 April 2023), 2(3):6, 2023.

Myung Jin Choi, Joseph J Lim, Antonio Torralba, and Alan S Willsky. Exploiting hierarchical context on a large database of object categories. In *2010 IEEE computer society conference on computer vision and pattern recognition*, pages 129–136. IEEE, 2010.

Xiangxiang Chu, Limeng Qiao, Xinyang Lin, Shuang Xu, Yang Yang, Yiming Hu, Fei Wei, Xinyu Zhang, Bo Zhang, Xiaolin Wei, et al. Mobilevlm: A fast, reproducible and strong vision language assistant for mobile devices. *arXiv preprint arXiv:2312.16886*, 1(2):3, 2023.

Yin Cui, Menglin Jia, Tsung-Yi Lin, Yang Song, and Serge Belongie. Class-balanced loss based on effective number of samples. In *Proceedings of the IEEE/CVF conference on computer vision and pattern recognition*, pages 9268–9277, 2019.

Damai Dai, Chengqi Deng, Chenggang Zhao, RX Xu, Huazuo Gao, Deli Chen, Jiashi Li, Wangding Zeng, Xingkai Yu, Y Wu, et al. Deepseekmoe: Towards ultimate expert specialization in mixture-of-experts language models. *arXiv preprint arXiv:2401.06066*, 2024.

Jacob Devlin, Ming-Wei Chang, Kenton Lee, and Kristina Toutanova. BERT: Pre-training of deep bidirectional transformers for language understanding. In Jill Burstein, Christy Doran, and Thamar Solorio, editors, *Proceedings of the 2019 Conference of the North American Chapter of the Association for Computational Linguistics: Human Language Technologies, Volume 1 (Long and Short Papers)*, pages 4171–4186, Minneapolis, Minnesota, June 2019. Association for Computational Linguistics. doi: 10.18653/v1/N19-1423. URL <https://aclanthology.org/N19-1423/>.

Alexey Dosovitskiy, Lucas Beyer, Alexander Kolesnikov, Dirk Weissenborn, Xiaohua Zhai, Thomas Unterthiner, Mostafa Dehghani, Matthias Minderer, Georg Heigold, Sylvain Gelly, et al. An image is worth 16x16 words: Transformers for image recognition at scale. *arXiv preprint arXiv:2010.11929*, 2020.

Shihan Dou, Enyu Zhou, Yan Liu, Songyang Gao, Jun Zhao, Wei Shen, Yuhao Zhou, Zhiheng Xi, Xiao Wang, Xiaoran Fan, et al. Loramoe: Revolutionizing mixture of experts for maintaining world knowledge in language model alignment. *arXiv preprint arXiv:2312.09979*, 2023.

Mathias Eitz, James Hays, and Marc Alexa. How do humans sketch objects? *ACM Transactions on graphics (TOG)*, 31(4):1–10, 2012.

Mark Everingham, Luc Van Gool, Christopher KI Williams, John Winn, and Andrew Zisserman. The pascal visual object classes (voc) challenge. *International journal of computer vision*, 88:303–338, 2010.

William Fedus, Barret Zoph, and Noam Shazeer. Switch transformers: Scaling to trillion parameter models with simple and efficient sparsity. *Journal of Machine Learning Research*, 23(120):1–39, 2022.

Chaoyou Fu, Peixian Chen, Yunhang Shen, Yulei Qin, Mengdan Zhang, Xu Lin, Jinrui Yang, Xiawu Zheng, Ke Li, Xing Sun, Yunsheng Wu, and Rongrong Ji. Mme: A comprehensive evaluation benchmark for multimodal large language models. *arXiv preprint arXiv:2306.13394*, 2023.

Tao Gong, Chengqi Lyu, Shilong Zhang, Yudong Wang, Miao Zheng, Qian Zhao, Kuikun Liu, Wenwei Zhang, Ping Luo, and Kai Chen. Multimodal-gpt: A vision and language model for dialogue with humans. *arXiv preprint arXiv:2305.04790*, 2023.

Yunhao Gou, Zhili Liu, Kai Chen, Lanqing Hong, Hang Xu, Aoxue Li, Dit-Yan Yeung, James T Kwok, and Yu Zhang. Mixture of cluster-conditional lora experts for vision-language instruction tuning. *arXiv preprint arXiv:2312.12379*, 2023.

Gregory Griffin, Alex Holub, Pietro Perona, et al. Caltech-256 object category dataset. Technical report, Technical Report 7694, California Institute of Technology Pasadena, 2007.

Yongxin Guo, Zhenglin Cheng, Xiaoying Tang, Zhaopeng Tu, and Tao Lin. Dynamic mixture of experts: An auto-tuning approach for efficient transformer models. *arXiv preprint arXiv:2405.14297*, 2024.

Suchin Gururangan, Mike Lewis, Ari Holtzman, Noah A Smith, and Luke Zettlemoyer. Demix layers: Disentangling domains for modular language modeling. *arXiv preprint arXiv:2108.05036*, 2021.

Hui Han, Wen-Yuan Wang, and Bing-Huan Mao. Borderline-smote: a new over-sampling method in imbalanced data sets learning. In *International conference on intelligent computing*, pages 878–887. Springer, 2005.

Kaiming He, Xiangyu Zhang, Shaoqing Ren, and Jian Sun. Deep residual learning for image recognition. In *Proceedings of the IEEE conference on computer vision and pattern recognition*, pages 770–778, 2016.

Youngkyu Hong, Seungju Han, Kwanghee Choi, Seokjun Seo, Beomsu Kim, and Buru Chang. Disentangling label distribution for long-tailed visual recognition. In *Proceedings of the IEEE/CVF conference on computer vision and pattern recognition*, pages 6626–6636, 2021.

Neil Houlsby, Andrei Giurgiu, Stanislaw Jastrzebski, Bruna Morrone, Quentin De Laroussilhe, Andrea Gesmundo, Mona Attariyan, and Sylvain Gelly. Parameter-efficient transfer learning for nlp. In *ICML*, pages 2790–2799. PMLR, 2019.

Edward J Hu, Yelong Shen, Phillip Wallis, Zeyuan Allen-Zhu, Yuanzhi Li, Shean Wang, Lu Wang, and Weizhu Chen. Lora: Low-rank adaptation of large language models. *arXiv preprint arXiv:2106.09685*, 2021.

Quzhe Huang, Zhenwei An, Nan Zhuang, Mingxu Tao, Chen Zhang, Yang Jin, Kun Xu, Liwei Chen, Songfang Huang, and Yansong Feng. Harder tasks need more experts: Dynamic routing in moe models. *arXiv preprint arXiv:2403.07652*, 2024.

Drew A Hudson and Christopher D Manning. Gqa: A new dataset for real-world visual reasoning and compositional question answering. In *Proceedings of the IEEE/CVF conference on computer vision and pattern recognition*, pages 6700–6709, 2019.

Robert A Jacobs, Michael I Jordan, Steven J Nowlan, and Geoffrey E Hinton. Adaptive mixtures of local experts. *Neural computation*, 3(1):79–87, 1991.

Yash Jain, Harkirat Behl, Zsolt Kira, and Vibhav Vineet. Damex: Dataset-aware mixture-of-experts for visual understanding of mixture-of-datasets. *Advances in Neural Information Processing Systems*, 36, 2024.

Mojan Javaheripi, Sébastien Bubeck, Marah Abdin, Jyoti Aneja, Sébastien Bubeck, Caio César Teodoro Mendes, Weizhu Chen, Allie Del Giorno, Ronen Eldan, Sivakanth Gopi, et al. Phi-2: The surprising power of small language models. *Microsoft Research Blog*, 1(3):3, 2023.

Yan Jin, Mengke Li, Yang Lu, Yiu-ming Cheung, and Hanzi Wang. Long-tailed visual recognition via self-heterogeneous integration with knowledge excavation. In *Proceedings of the IEEE/CVF conference on computer vision and pattern recognition*, pages 23695–23704, 2023.

Bingyi Kang, Yu Li, Sa Xie, Zehuan Yuan, and Jiashi Feng. Exploring balanced feature spaces for representation learning. In *International conference on learning representations*, 2020.

Wonjae Kim, Bokyung Son, and Ildoo Kim. Vilt: Vision-and-language transformer without convolution or region supervision. In *International conference on machine learning*, pages 5583–5594. PMLR, 2021.

Alex Krizhevsky, Ilya Sutskever, and Geoffrey E Hinton. Imagenet classification with deep convolutional neural networks. *Communications of the ACM*, 60(6):84–90, 2017.

Hugo Laurençon, Lucile Saulnier, Léo Tronchon, Stas Bekman, Amanpreet Singh, Anton Lozhkov, Thomas Wang, Siddharth Karamcheti, Alexander Rush, Douwe Kiela, et al. Obelics: An open web-scale filtered dataset of interleaved image-text documents. *Advances in Neural Information Processing Systems*, 36: 71683–71702, 2023.

Dmitry Lepikhin, HyoukJoong Lee, Yuanzhong Xu, Dehao Chen, Orhan Firat, Yanping Huang, Maxim Krikun, Noam Shazeer, and Zhifeng Chen. Gshard: Scaling giant models with conditional computation and automatic sharding. *arXiv preprint arXiv:2006.16668*, 2020.

Brian Lester, Rami Al-Rfou, and Noah Constant. The power of scale for parameter-efficient prompt tuning. *arXiv preprint arXiv:2104.08691*, 2021.

Bo Li, Yifei Shen, Jingkang Yang, Yezhen Wang, Jiawei Ren, Tong Che, Jun Zhang, and Ziwei Liu. Sparse mixture-of-experts are domain generalizable learners. *arXiv preprint arXiv:2206.04046*, 2022.

Da Li, Yongxin Yang, Yi-Zhe Song, and Timothy M Hospedales. Deeper, broader and artier domain generalization. In *Proceedings of the IEEE international conference on computer vision*, pages 5542–5550, 2017.

Yifan Li, Yifan Du, Kun Zhou, Jinpeng Wang, Wayne Xin Zhao, and Ji-Rong Wen. Evaluating object hallucination in large vision-language models. *arXiv preprint arXiv:2305.10355*, 2023.

Bin Lin, Zhenyu Tang, Yang Ye, Jiaxi Cui, Bin Zhu, Peng Jin, Junwu Zhang, Munan Ning, and Li Yuan. Moe-llava: Mixture of experts for large vision-language models. *arXiv preprint arXiv:2401.15947*, 2024a.

Tsung-Yi Lin, Michael Maire, Serge Belongie, James Hays, Pietro Perona, Deva Ramanan, Piotr Dollár, and C Lawrence Zitnick. Microsoft COCO: Common objects in context. In *ECCV*, 2014.

Tsung-Yi Lin, Priya Goyal, Ross Girshick, Kaiming He, and Piotr Dollár. Focal loss for dense object detection. In *Proceedings of the IEEE international conference on computer vision*, pages 2980–2988, 2017.

Xi Victoria Lin, Akshat Shrivastava, Liang Luo, Srinivasan Iyer, Mike Lewis, Gargi Ghosh, Luke Zettlemoyer, and Armen Aghajanyan. Moma: Efficient early-fusion pre-training with mixture of modality-aware experts. *arXiv preprint arXiv:2407.21770*, 2024b.

Haotian Liu, Chunyuan Li, Yuheng Li, and Yong Jae Lee. Improved baselines with visual instruction tuning. *arXiv preprint arXiv:2310.03744*, 2023a.

Yuan Liu, Haodong Duan, Yuanhan Zhang, Bo Li, Songyang Zhang, Wangbo Zhao, Yike Yuan, Jiaqi Wang, Conghui He, Ziwei Liu, et al. Mmbench: Is your multi-modal model an all-around player? *arXiv preprint arXiv:2307.06281*, 2023b.

Ziwei Liu, Zhongqi Miao, Xiaohang Zhan, Jiayun Wang, Boqiang Gong, and Stella X Yu. Large-scale long-tailed recognition in an open world. In *Proceedings of the IEEE/CVF conference on computer vision and pattern recognition*, pages 2537–2546, 2019.

Haoyu Lu, Wen Liu, Bo Zhang, Bingxuan Wang, Kai Dong, Bo Liu, Jingxiang Sun, Tongzheng Ren, Zhusu Li, Hao Yang, Yaofeng Sun, Chengqi Deng, Hanwei Xu, Zhenda Xie, and Chong Ruan. Deepseek-vl: Towards real-world vision-language understanding, 2024.

Pan Lu, Swaroop Mishra, Tanglin Xia, Liang Qiu, Kai-Wei Chang, Song-Chun Zhu, Oyvind Tafjord, Peter Clark, and Ashwin Kalyan. Learn to explain: Multimodal reasoning via thought chains for science question answering. *Advances in Neural Information Processing Systems*, 35:2507–2521, 2022.

Jiaqi Ma, Zhe Zhao, Xinyang Yi, Jilin Chen, Lichan Hong, and Ed H Chi. Modeling task relationships in multi-task learning with multi-gate mixture-of-experts. In *Proceedings of the 24th ACM SIGKDD international conference on knowledge discovery & data mining*, pages 1930–1939, 2018.

Aditya Krishna Menon, Sadeep Jayasumana, Ankit Singh Rawat, Himanshu Jain, Andreas Veit, and Sanjiv Kumar. Long-tail learning via logit adjustment. *arXiv preprint arXiv:2007.07314*, 2020.

MetaAI. Llama 3 on groq: Achieving unprecedented token generation speeds with integration on groq cloud. 2024. URL <https://llama-2.ai/llama-3-on-groq/>.

Huy Nguyen, Xing Han, Carl William Harris, Suchi Saria, and Nhat Ho. On expert estimation in hierarchical mixture of experts: Beyond softmax gating functions. *arXiv preprint arXiv:2410.02935*, 2024.

Xingchao Peng, Qinxun Bai, Xide Xia, Zijun Huang, Kate Saenko, and Bo Wang. Moment matching for multi-source domain adaptation. In *Proceedings of the IEEE/CVF international conference on computer vision*, pages 1406–1415, 2019.

Alec Radford, Jong Wook Kim, Chris Hallacy, Aditya Ramesh, Gabriel Goh, Sandhini Agarwal, Girish Sastry, Amanda Askell, Pamela Mishkin, Jack Clark, et al. Learning transferable visual models from natural language supervision. In *International conference on machine learning*, pages 8748–8763. PMLR, 2021.

Nils Reimers and Iryna Gurevych. Sentence-bert: Sentence embeddings using siamese bert-networks. *arXiv preprint arXiv:1908.10084*, 2019.

Jiawei Ren, Cunjun Yu, Xiao Ma, Haiyu Zhao, Shuai Yi, et al. Balanced meta-softmax for long-tailed visual recognition. *Advances in neural information processing systems*, 33:4175–4186, 2020.

Bryan C Russell, Antonio Torralba, Kevin P Murphy, and William T Freeman. Labelme: a database and web-based tool for image annotation. *International journal of computer vision*, 77:157–173, 2008.

Patsorn Sangkloy, Nathan Burnell, Cusuh Ham, and James Hays. The sketchy database: learning to retrieve badly drawn bunnies. *ACM Transactions on Graphics (TOG)*, 35(4):1–12, 2016.

Noam Shazeer, Azalia Mirhoseini, Krzysztof Maziarz, Andy Davis, Quoc Le, Geoffrey Hinton, and Jeff Dean. Outrageously large neural networks: The sparsely-gated mixture-of-experts layer. *arXiv preprint arXiv:1701.06538*, 2017.

Amanpreet Singh, Vivek Natarajan, Meet Shah, Yu Jiang, Xinlei Chen, Dhruv Batra, Devi Parikh, and Marcus Rohrbach. Towards vqa models that can read. In *Proceedings of the IEEE/CVF conference on computer vision and pattern recognition*, pages 8317–8326, 2019.

Hugo Touvron, Thibaut Lavigra, Gautier Izacard, Xavier Martinet, Marie-Anne Lachaux, Timothée Lacroix, Baptiste Rozière, Naman Goyal, Eric Hambro, Faisal Azhar, et al. Llama: Open and efficient foundation language models. *arXiv preprint arXiv:2302.13971*, 2023.

Ashish Vaswani, Noam Shazeer, Niki Parmar, Jakob Uszkoreit, Llion Jones, Aidan N Gomez, Łukasz Kaiser, and Illia Polosukhin. Attention is all you need. *Advances in neural information processing systems*, 30, 2017.

Hemanth Venkateswara, Jose Eusebio, Shayok Chakraborty, and Sethuraman Panchanathan. Deep hashing network for unsupervised domain adaptation. In *Proceedings of the IEEE conference on computer vision and pattern recognition*, pages 5018–5027, 2017.

Xudong Wang, Long Lian, Zhongqi Miao, Ziwei Liu, and Stella X Yu. Long-tailed recognition by routing diverse distribution-aware experts. *arXiv preprint arXiv:2010.01809*, 2020.

Yu-Xiong Wang, Deva Ramanan, and Martial Hebert. Learning to model the tail. *Advances in neural information processing systems*, 30, 2017.

Longrong Yang, Dong Shen, Chaoxiang Cai, Fan Yang, Size Li, Di Zhang, and Xi Li. Solving token gradient conflict in mixture-of-experts for large vision-language model. *arXiv preprint arXiv:2406.19905*, 2024.

Qinghao Ye, Haiyang Xu, Guohai Xu, Jiabo Ye, Ming Yan, Yiyang Zhou, Junyang Wang, Anwen Hu, Pengcheng Shi, Yaya Shi, et al. mplug-owl: Modularization empowers large language models with multimodality. *arXiv preprint arXiv:2304.14178*, 2023.

Weihao Yu, Zhengyuan Yang, Linjie Li, Jianfeng Wang, Kevin Lin, Zicheng Liu, Xinchao Wang, and Lijuan Wang. Mm-vet: Evaluating large multimodal models for integrated capabilities. *arXiv preprint arXiv:2308.02490*, 2023.

Zhengqing Yuan, Zhaoxu Li, Weiran Huang, Yanfang Ye, and Lichao Sun. Tinygpt-v: Efficient multimodal large language model via small backbones. *arXiv preprint arXiv:2312.16862*, 2023.

Yanzhe Zhang, Ruiyi Zhang, Jiuxiang Gu, Yufan Zhou, Nedim Lipka, Diyi Yang, and Tong Sun. Llavar: Enhanced visual instruction tuning for text-rich image understanding. *arXiv preprint arXiv:2306.17107*, 2023.

Zexuan Zhong, Mengzhou Xia, Danqi Chen, and Mike Lewis. Lory: Fully differentiable mixture-of-experts for autoregressive language model pre-training. *arXiv preprint arXiv:2405.03133*, 2024.

Yuhang Zhou, Zihua Zhao, Haolin Li, Siyuan Du, Jiangchao Yao, Ya Zhang, and Yanfeng Wang. Exploring training on heterogeneous data with mixture of low-rank adapters. *arXiv preprint arXiv:2406.09679*, 2024.

Yichen Zhu, Minjie Zhu, Ning Liu, Zhiyuan Xu, and Yixin Peng. Llava-phi: Efficient multi-modal assistant with small language model. In *Proceedings of the 1st International Workshop on Efficient Multimedia Computing under Limited*, pages 18–22, 2024.

Supplementary Material

In our supplementary material, we provide the following details and experiments:

- A: We provide the implementation detail about experiments.
- B: We provide more comparison study experiments.
- C: We statistic the expert token loading.

A Implementation Details

A.1 Instruction Tuning Dataset and Benchmarks

Instruction Tuning Dataset. We employ the LLaVA-mix-665k dataset Liu et al. [2023a] as the instruction tuning data for our vision-language tasks. The structure and composition of the dataset are shown in Tab. 8.

Table 8: **Instruction-following data mixture.** The data is from LLaVA-1.5 Liu et al. [2023a].

Data	Size	Response formatting prompts
LLaVA	158K	-
ShareGPT	40K	-
VQAv2	83K	
GQA	72K	
OKVQA	9K	Answer the question using a single word or phrase.
OCRVQA	80K	
A-OKVQA	66K	Answer with the option’s letter from the given choices directly.
TextCaps	22K	Provide a one-sentence caption for the provided image.
RefCOCO	48K	Provide a short description for this region.
VG	86K	Provide the bounding box coordinate of the region this sentence describes.
Total	665K	

Benchmarks. We utilize the vision-language benchmarks of MoE-LLaVA Lin et al. [2024a] and the vison-only benchmarks of GMoE Li et al. [2022]. The detail benchmarks description are shown in Tab. 9. These benchmarks provide a comprehensive evaluation framework, ensuring rigorous test across diverse capabilities.

A.2 Training Configurations

Our training configurations is based on the MoE-LLaVA Lin et al. [2024a] and GMoE Li et al. [2022], with detailed implementations in Tab. 10. In the instruction fine-tuning phase of MoE-LLaVA, we employ a batch size of 128 and a learning rate of 2e-5. We also use the pre-trained models of MoE-LLaVA³.

A.3 Routing Strategies

TASK, CLUSTER, INSTRUCT, DYNAMIC, and STGC denote task routing Gururangan et al. [2021], Jain et al. [2024], Zhou et al. [2024], cluster routing Dou et al. [2023], Gou et al. [2023], instruction routing Chen et al. [2023a], dynamic routing Huang et al. [2024], Guo et al. [2024], and conflicts mitigation routing Yang et al. [2024], respectively. Our detailed implements are illustrated as follows:

1. **TASK.** Similar to MoLA Zhou et al. [2024], aims to enhance similar routing for data from the same task while ensure distinct routing for data from different tasks. We conduct experiments using the LLaVA-mix-665k dataset, which is significantly different from the

³<https://huggingface.co/openai/clip-vit-large-patch14-336>; <https://github.com/haotian-liu/LLaVA>.

Table 9: Our benchmarks on both vision-language and vision-only.

Vision-Language Benchmarks	
Benchmark	Description
GQA Hudson and Manning [2019]	For visual perception capabilities of models through open-ended short answers.
ScienceQA Lu et al. [2022]	For zero-shot generalization of models on scientific question answering.
TextVQA Singh et al. [2019]	For text-rich visual question answering tasks.
POPE Li et al. [2023]	For degree of hallucination in model responses on three sampled subsets of COCO Lin et al. [2014].
MME Fu et al. [2023]	For visual perception of models with yes/no questions.
MMBench Liu et al. [2023b]	For robustness of model answers with all-round shuffling on multiple choice answers.
MM-Vet Yu et al. [2023]	For model capabilities in engaging in visual conversations on a diverse range of tasks and evaluates the correctness and helpfulness of the responses using the GPT-4 evaluation framework.
Vision-Only Benchmarks	
Benchmark	Description
PACS Li et al. [2017]	Consists of intersecting classes from Caltech256, Sketchy401 Sangkloy et al. [2016], TU-Berlin Eitz et al. [2012], and Google Images, providing a diverse set of visual domains.
VLCS Albuquerque et al. [2019]	Combines examples from five overlapping classes across VOC2007 Everingham et al. [2010], LabelMe Russell et al. [2008], Caltech-101 Griffin et al. [2007], and SUN Choi et al. [2010], offering a broad evaluation of cross-domain generalization.
Office-Home Venkateswara et al. [2017]	Contains approximately 15,500 images organized into 65 categories across four domains, making it suitable for assessing domain adaptation algorithms.
DomainNet Peng et al. [2019]	For the need of multi-source unsupervised domain adaptation research, featuring six domains and around 0.6 million images distributed across 345 categories.

Table 10: Training Hyper-parameters.

Epoch	Learning Rate	Learning Rate Schedule	Weight Decay	Load Balancing Loss Coefficient
1	2e-5	Cosine	0.0	0.01
Text Max Length	Batch Size per GPU	GPU	Precision	The Number of a in EEA
2048	16	8 × A800-80G	Fp16	4

data used in MoLA. Empirically, we categorize the data into four task types: (1) *Caption*, where the instruction might be "provide a one-sentence caption for the provided image.>"; (2) *VQA*, with instructions like "answer the question using a single word or phrase.>"; (3) *OCR*, which includes all data from OCRVQA; and (4) *Region-aware*, where the instruction could be "provide a short description for this region." Each task type is assigned an expert label: 0 for *Caption*, 1 for *VQA*, 2 for *OCR*, and 3 for *Region-aware*. The dataset distributions are: *Caption* accounts for 3.5%, *VQA* for 61.6%, *OCR* for 12.8%, and *Region-aware* for 22.1%.

2. **CLUSTER**. Following the methodology of MoCLE Gou et al. [2023], we encode all instructions from different datasets using the all-MiniLM-L6-v2⁴ variant of the Sentence Transformer model Reimers and Gurevych [2019] and cluster their embeddings using the k -means clustering algorithm. After clustering, in line with MoCLE's approach, we initialize K learnable embeddings, where each embedding corresponds to a cluster center. When a sample belongs to the k -th cluster center, the k -th learnable embedding is extracted and passed to the router to predict routing scores. We set k -th=128, consistent with MoCLE's practice, and do not incorporate the load balance loss.
3. **INSTRUCT**. Following the approach of LoRA-MoE Chen et al. [2023a], we compute the average of instruction token representations for each instance and use this as input to predict its routing scores across experts. Based on these routing scores, the Top- k experts are selected for each sample to generate the final prediction. In alignment with LoRA-MoE's methodology, we do not include the load balance loss in our implementation.
4. **DYNAMIC**. Drawing inspiration from DYNMOE Guo et al. [2024], we highlight its innovative gating mechanism, which allows each token to dynamically determine the number of

⁴<https://huggingface.co/sentence-transformers/all-MiniLM-L6-v2>.

experts to activate. Additionally, an adaptive process automatically adjusts the number of experts during training. We reference its experimental results on the MoE-LLaVA-4Top2 with StableLM-1.6B model, where an average of 1.25 experts out of 4 are activated per token.

5. **STGC**. STGC Yang et al. [2024] employs token-level gradients to identify conflicting tokens within experts. Additionally, it introduces a regularization loss designed to encourage conflicting tokens to route away from their current experts to alternative ones, thereby minimizing interference among tokens within the same expert. We reference their experimental results on the MoE-LLaVA-4Top2 using the StableLM-1.6B model.

B More Comparison Study Experiments

B.1 Comparison with Modality-aware MoE Framework

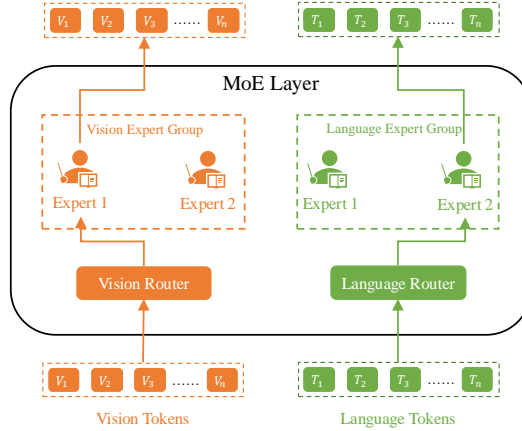


Figure 3: **The overview of the modality-aware MoE framework which divides experts for vision and language TER, respectively.**

To compare with existing modality-aware MoE frameworks as shown in Fig. 3, such as Chen et al. [2024a], Lin et al. [2024b], Nguyen et al. [2024], we adopt the following configurations:

1. **MoE-LLaVA-1.6B-v2Top1-t2Top1**. We partition experts into two groups dedicated to vision and language, respectively. As illustrated in Fig.3, to maintain the total number of experts K (set to 4 in this study) and the number of activated experts k (set to 2 in this study), we designate 2 experts as vision experts and the remaining 2 as language experts, activating 1 expert from each modality group.
2. **MoE-LLaVA-1.6B-v4Top2-t4Top2**. We first expand the 4 experts into 8 by splitting FFN intermediate hidden dimension Dai et al. [2024], assigning 4 as vision experts and the remaining 4 as language experts, and activating 2 experts from each modality group.
3. **MoE-LLaVA-1.6B-v2Top1-t2Top1-DAR**. This configuration is similar to *MoE-LLaVA-1.6B-v2Top1-t2Top1*, but it removes the expert load balancing constraint for the vision expert group (similar to the distribution-aware router in our proposed approach, LTDR).
4. **MoE-LLaVA-1.6B-v2Top1-t2Top1-DAR-shared**. This setup is akin to *MoE-LLaVA-1.6B-v2Top1-t2Top1-DAR*, but it includes a shared expert for learning world knowledge Dai et al. [2024].

The results in Tab.11 indicate that the modality-aware MoE does not enhance the performance of LVLMs. Moreover, increasing the number of experts results in a significant performance decline, suggesting that a larger number of experts exacerbates expert load balancing issues, which negatively impacts vision TER. When the expert load balancing constraint is removed for the vision expert group, *MoE-LLaVA-1.6B-v2Top1-t2Top1-DAR* shows improved performance compared to MoE-LLaVA-4Top2, validating the effectiveness of our DAR approach. Finally, the addition of an extra expert in

Table 11: **Comparison with a series of modality-aware MoE framework settings.** Chen et al. [2024a], Lin et al. [2024b], Nguyen et al. [2024] All experiments are conducted on the MoE-LLaVA-4Top2 with StableLM-1.6B model.

Method	GQA	SQA ^T	VQA ^T	POPE	MME	MMB	MM-Vet	Avg
MoE-LLaVA-4Top2	60.3*	62.6	50.1	85.7	1318.2	60.2	26.9	57.6
<i>Modality-aware MoE</i>								
MoE-LLaVA-1.6B-v2Top1-t2Top1	60.4*	61.6	49.2	85.9	1293.3	61.1	28.4	57.7
MoE-LLaVA-1.6B-v4Top2-t4Top2	60.3*	58.6	46.8	85.7	1296.6	55.4	26.4	55.5
MoE-LLaVA-1.6B-v2Top1-t2Top1-DAR	60.9*	61.3	51.0	86.5	1324.5	61.1	28.4	58.2
MoE-LLaVA-1.6B-v2Top1-t2Top1-DAR-shared	61.0*	62.5	51.3	86.5	1333.8	60.0	28.0	58.2
Our Method	61.1*	63.4	51.1	86.6	1363.5	60.6	29.9	58.8

MoE-LLaVA-1.6B-v2Top1-t2Top1-DAR-shared does not yield benefits, highlighting the distinctions between vision-language MoE and language-only MoE Dai et al. [2024].

B.2 Object Hallucination Evaluation

Table 12: **Zero-shot object hallucination evaluation results.** “L”, “V” and “S” respectively represent LLaMA Touvron et al. [2023], Vicuna Chiang et al. [2023] and StableLM Bellagente et al. [2024]. All “Sparse Model” methods use the configure 4Top2.

Method	LLM	Adversarial			Popular			Random		
		Acc	F1-Score	Yes	Acc	F1-Score	Yes	Acc	F1-Score	Yes
<i>Dense Model</i>										
mPLUG-Owl Ye et al. [2023]	L-7B	82.4	81.6	45.2	85.5	84.3	42.1	86.3	85.3	42.3
MM-GPT Gong et al. [2023]	L-7B	50.0	66.7	100.0	50.0	66.7	100.0	50.0	66.7	100.0
LLaVA-1.5 Liu et al. [2023a]	V-13B	85.5	84.4	43.3	87.4	86.2	41.3	88.0	87.1	41.7
<i>Sparse Model</i>										
MoE-LLaVA-1.6Bx4-Top2 Ye et al. [2023]	S-1.6B	86.9	85.7	41.7	85.3	84.2	43.5	88.0	87.1	41.6
Our Method Ye et al. [2023]	S-1.6B	85.8	84.2	43.3	86.5	86.0	41.4	88.0	87.2	41.3

We employ the evaluation pipeline of POPE Li et al. [2023], a polling-based query methodology, to assess object hallucination in MoE-LLaVA. As shown in Tab. 12, our proposed method demonstrates superior performance compared to baseline approaches, suggesting its enhanced capability in generating object descriptions that are more consistent with the visual content of the given images.

C Expert Token Loading

We analyze the distribution of expert token loading across all MoE layers on GQA Hudson and Manning [2019]. As depicted in Fig.4, MoE-LLaVA serves as the baseline model, MoE-LLaVA-LB denotes the MoE-LLaVA without language load balancing, and MoE-LLaVA+LTDR denotes the MoE-LLaVA with LTDR. The figure shows that language tokens consistently follows a uniform distribution. In contrast, LTDR eliminates vision load balancing, the imbalanced distribution of vision tokens shows that more vision tokens select specialized experts. This supports our hypothesis that the TER for language tokens adheres to a uniform distribution, whereas the TER for vision tokens follows a long-tailed distribution.

We also compare the token routing probability variance (RPV) between vision head tokens and vision tail tokens across GQA Hudson and Manning [2019], MMBench Liu et al. [2023b] and TextVQA Singh et al. [2019]. As illustrated in Fig. 5, for images that yield 576 tokens from CLIP, $\text{Mean}(\text{RPV}(\mathcal{V}))$ denotes the mean RPV of all vision tokens \mathcal{V} , $\mathcal{V}_{\text{head}}$ and $\mathcal{V}_{\text{tail}}$ denote vision head tokens and vision tail tokens. The bars in the figure is the mean token count with RPV ranging from left to right for images (e.g., in the upper left figure, the count of tokens with RPV ranging from 0.00 to 0.01 is 442). Our method significantly increases the mean RPV of vision tail tokens. Given that RPV reflects the TER probability distribution, these results demonstrate that vision tail tokens gain the ability to select their specialized experts. Meanwhile, the mean RPV of vision head tokens remains nearly unchanged, indicating that vision head tokens are not affected.

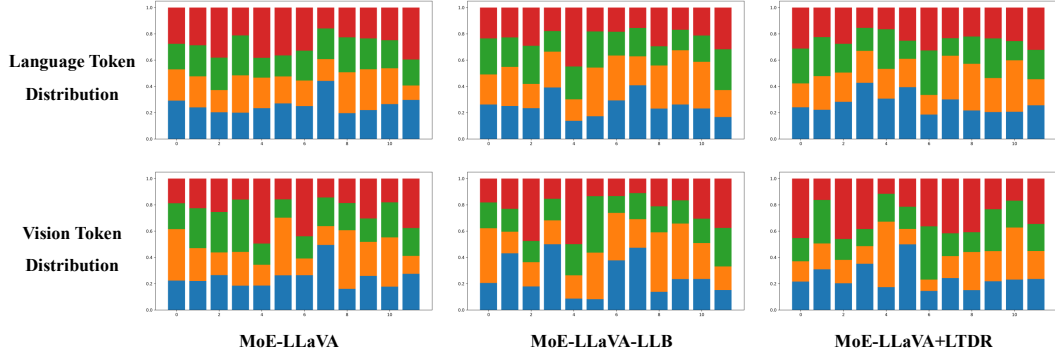


Figure 4: Expert Token Loading on GQA.

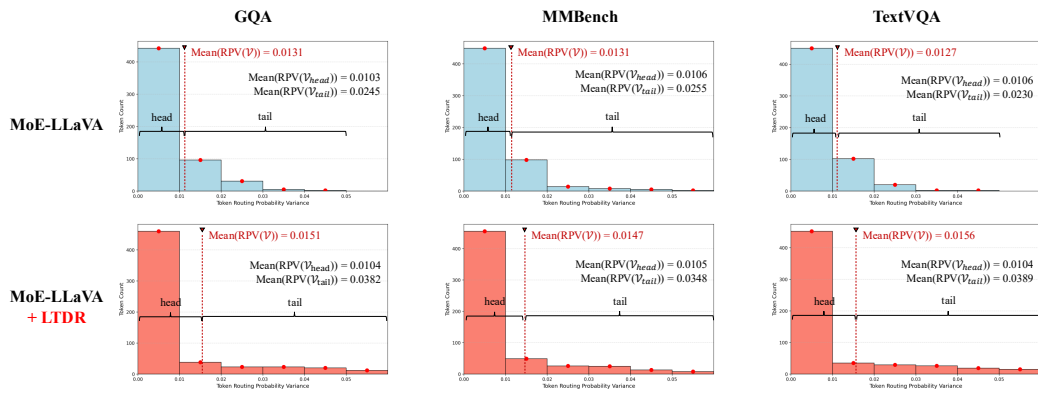


Figure 5: The Routing Probability Variance between Vision Head Tokens and Vision Tail Tokens across three benchmarks.